

RESEARCH LETTER

Open Access



Active sediment transport along trench axis: insights from X-ray fluorescence core scanning and magnetic analysis of marine sediments in the southwestern Ryukyu Trench

Kan-Hsi Hsiung^{1*} , Toshiya Kanamatsu¹, Ken Ikehara², Masafumi Murayama³ and Yuhji Yamamoto⁴

Abstract

The southwestern Ryukyu Trench is an ideal place for investigating sediment transport from the Taiwan mountain belt to the Ryukyu Trench floor. To study the characteristics of trench turbidites and sediment transport along the trench, we utilize two piston cores: KR1518-PC04/PL04 at the southwestern end of Ryukyu Trench and YK1501-PC14/PL14 in the trench floor. We also collect two push cores, YK1611-6K1467MG and 6K1467MR, from undisturbed seabed surface to observe lithology. Our analysis reveals that the lithology of the cores shows homogeneous gray mud layers intercalated with very-thin fine sand layers, which we interpret as hemipelagites intercalated with very-thin turbidites. We identify 60 turbidites (0.3–4.0 cm thick) from YK1501-PC14 and 36 turbidites (0.9–4.2 cm thick) from KR1518-PC04. Based on observation from YK1501-PC14, most turbidites, which were less than 1 cm in thickness, displayed planar and sharp bottom contacts. The turbidite thickness of YK1501-PC14 (6448 m water depth) is thinner than that of KR1518-PC04 (6147 m water depth) in general. Through X-ray fluorescence core scans (ITRAX), we distinguished trench turbidites by elemental patterns and accurately determined the depths of every very-thin turbidite. Most hemipelagites from YK1501-PC14 and KR1518-PC04 show similar ITRAX profiles, indicating a similar source of the sediments. ITRAX analysis also revealed five intervals in high-Ca mud in YK1501-PC14, suggesting another potential source from the Ryukyu forearc. Anisotropy of Magnetic Susceptibility (AMS) results show that both YK1501-PC14/PL14 and KR1518-PC04/PL04 exhibit an oblate fabric indicating a normal sedimentary condition. Magnetic signatures showed the presence of pyrrhotite, supporting evidence that Taiwan-sourced sediments can be transported up to ~250 km by turbidity currents and spread from the Taiwan Island to the Ryukyu Trench floor. This study improves our understanding of Ryukyu Trench turbidites and provides valuable insights into active sediment transport along the southwestern Ryukyu Trench.

Keywords Trench turbidites, Anisotropy of magnetic susceptibility, Pyrrhotite, ITRAX, Ryukyu Trench, Taiwan

*Correspondence:

Kan-Hsi Hsiung
hsiung@jamstec.go.jp

Full list of author information is available at the end of the article

Background

Hadal trenches (>6000 m water depth) comprise only ~1% of the world's ocean floor and remain largely unexplored. Fortunately, increasing attention has been given to the transport and accumulation of hadal sediments (e.g., Ikehara et al. 2018; Oguri et al. 2022). Oceanic trench sediment studies are crucial for gaining important insights into the dynamic processes that occur in the deepest parts of the ocean floor. Trench sedimentation has large variability in depositional style within trench environments. Generally, trench-filling sediments are transported downslope from adjacent forearc ridges by gravity-driven sediment flows, whereas axial sediment transport via submarine canyons and channels plays an important role in delivering terrigenous sediments from distant areas to the trench floor (e.g., Malatesta et al. 2013; Pickering and Hiscott 2015; Hsiung et al. 2017). For example, the southwestern Ryukyu Trench is considered to be a sediment sink containing large amounts of sediment along the trench floor (Malatesta et al. 2013).

In the tectonic setting view, the formation of the Ryukyu Island Arc north of the southwestern Ryukyu Trench resulted from the subduction of the Philippine Sea Plate beneath the Eurasia Plate (Karig 1973; Angelier 1986). Previous studies have inferred a slide mass in accretionary prism collapse (Okamura et al. 2018) and tsunami-induced sediment transport from Coral Reef to the southern Ryukyu forearc (Ikehara et al. 2022), suggesting the possibility of sources from the Ryukyu forearc. Using detrital pyrrhotite as a tracer, eroded from the metamorphic terranes of Taiwan's Central Range, sediments can be transported eastward to the southwestern Ryukyu Trench end, serving as a diagnostic tracer for sediment transport from source to sink (Horng and Huh 2011; Horng et al. 2012; Hsiung et al. 2021). Accordingly, the Ryukyu forearc and Taiwan are considered potential sediment supply sources for the southwestern Ryukyu Trench.

The transport and accumulation of sediment material of the Ryukyu Trench remain poorly understood. To address this, our study focuses on analyzing the newly introduced a piston core YK1501-PC14/PL14, in conjunction with previously reported one piston core KR1518-PC04/PL04 (Hsiung et al. 2021) and two push cores YK1611-6K1467MG/6K1467MR (Kawamura et al. 2023). Our goal is to provide evidence of sediment transport and enhance our understanding of discrepancies of turbidites along the southwestern Ryukyu Trench floor. The analysis of KR1518-PC04/PL04 suggests that Taiwan-sourced sediments can be transported into the Huatung Basin and the end of southwestern Ryukyu Trench primarily by turbidity currents through submarine canyons (Hsiung et al. 2017, 2021). Sites KR1518-PC04/PL04

are at the southwestern end of the Ryukyu Trench, while YK1501-PC14/PL14 is located in a terminal fan where the deep-sea channel ends, about 100 km apart (Fig. 1). These sites resemble wide fan-shaped river mouths, extending from upstream levees to broader downstream areas. North of YK1501-PC14/PL14, YK1611-6K1467MG is about 2.3 km away, and YK1611-6K1467MR is 1.8 km north of 6K1467MG (Fig. 1c). The cruise names of cores will be omitted hereafter.

Materials and methods

Bathymetry and core collection

Previous research showed that the Hualien Canyon at the Huatung Basin and channel-terminal fan system at the southwestern Ryukyu Trench provide a longitudinal pathway for far-field sediment transport (Hsiung et al. 2017; 2021). Swath bathymetric data used in this study were collected in 2015 during JAMSTEC cruises YK1501 by *R/V Yokosuka* and KR1518 by *R/V Kairei* (JAMSTEC 2015, 2016). Piston cores PC14/PL14 were obtained at a water depth of 6448 m on the trench floor at 23° 12.0169 N, 124° 08.9843 E during cruise YK1501 (Additional file 1: Table S1). In between the sites PC04/PL04 and PC14/PL14, a submarine channel extending ~100 km from the Hualien Canyon mouth into the southwestern Ryukyu Trench. Farther eastward, the submarine channel culminated in a radial pattern and connected to a submarine fan structure that can be considered as a trench basin elongated over a width of ~30 km (Fig. 1). An 8 m-long piston coring system with 7.8 cm-diameter core liners was used to collect piston core PC14 and gravity pilot core PL14, with PC14 measuring 263.0 cm in length and PL14 measuring 24.0 cm. The cores were split laterally onboard and physically described, and X-ray images were taken of slab samples (1 cm thick and 20 cm long) to observe sedimentary structures in detail. The results of PC14/PL14 are further discussed with previous cores, including cores PC04/PL04 and 6K1467MG from the flat seafloor, and 6K1467MR from the landward trench slope (Fig. 1c).

XRF core scanning profiles

The XRF core scanning was measured at the Kochi Core Center using the ITRAX XRF Core Scanner (hereafter ITRAX), which is manufactured by Cox Analytical Systems. The ITRAX system uses an X-ray beam (0.2×20 mm) to excite the samples, generating radiographic images and energy dispersive XRF spectra (Croudace et al. 2006; Löwemark et al. 2019). We employed a high resolution for the scanning process, setting the scanning step size to 0.05 cm, which is particularly beneficial for capturing very thin event layers,

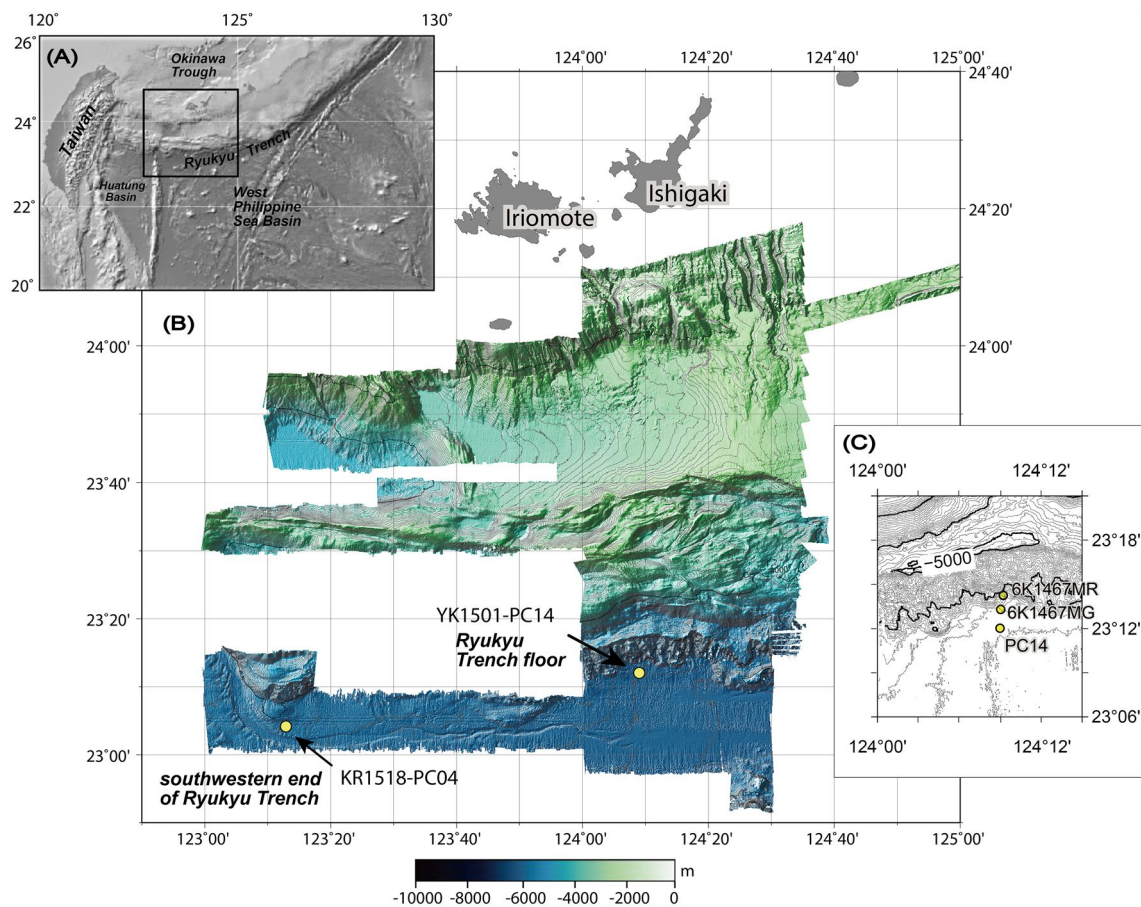


Fig. 1 Detailed bathymetry and core sites in the southwestern Ryukyu Trench. **a** Upper left box shows location of the study area (black square). **b** Piston cores KR1518-PC04/PL04 are in the southwestern end of Ryukyu Trench. The site YK1501-PC14/PL14, southwestern Ryukyu Trench floor, is ~100 km east of the site KR1518-PC04/PL04. **c** The sites 6K1467MG and 6K1467MR of YK1611 are located near YK1501-PC14. Check the latitude and longitude in Additional file 1: Table S1

as most of them are less than 1 cm in thickness. The elemental compositions from ITRAX are semiquantitative relative to elemental intensities, reported as counts, and were calculated as five-point running averages. The target elements analyzed from ITRAX include Ca, Sr, Zr, Si, Mn, Fe, Ti, K, Rb, and Zn (Fig. 2). This study also includes part of the other ITRAX data from cores PC04/PL04 (Hsiung et al. 2021), 6K1467MG, and 6K1467MG (Kawamura et al. 2023). In PC04/PL04, the Ca/Fe and Zr/Rb ratios of ITRAX were used to identify distal turbidites (~1–3 cm thick), while Zr/Rb peaks primarily reflect grain size changes (Hsiung et al. 2021). The cores 6K1467MG and 6K1467MR have been analyzed for ITRAX element profiles, including Ca, K, Mn, and Al (Kawamura et al. 2023), with selected element profiles provided to support the lithological description of the comparable turbidites (Additional file 4: Fig. S1).

Magnetic parameters

Samples for magnetic fabric analyses were encased in 7 cm³ plastic cubes at 2.2 cm intervals spanning the entire cores and analyzed using a KLY-4 magnetic susceptibility meter (AGICO Inc.) for anisotropy of magnetic susceptibility (AMS) measurements. A total of 113 cubes from PC14 and 10 cubes from PL14 were measured in JAMSTEC Yokosuka headquarters, Japan. Besides, the results of PC04/PL04 including 145 cubes from PC04 and 33 cubes from PL04 were discussed together in the later section (Hsiung et al. 2021). We used the following parameters: P (degree of anisotropy) = K_{\max}/K_{\min} , F (degree of foliation) = K_{int}/K_{\min} , L (degree of lineation) = K_{\max}/K_{int} , T (shape parameter) = $[\ln F - \ln L]/[\ln F + \ln L]$, and K_m (Mean magnetic susceptibility).

Detrital pyrrhotite, a useful tracer for studying sediment transport processes from terrestrial landmasses to submarine basins, may have been episodically eroded

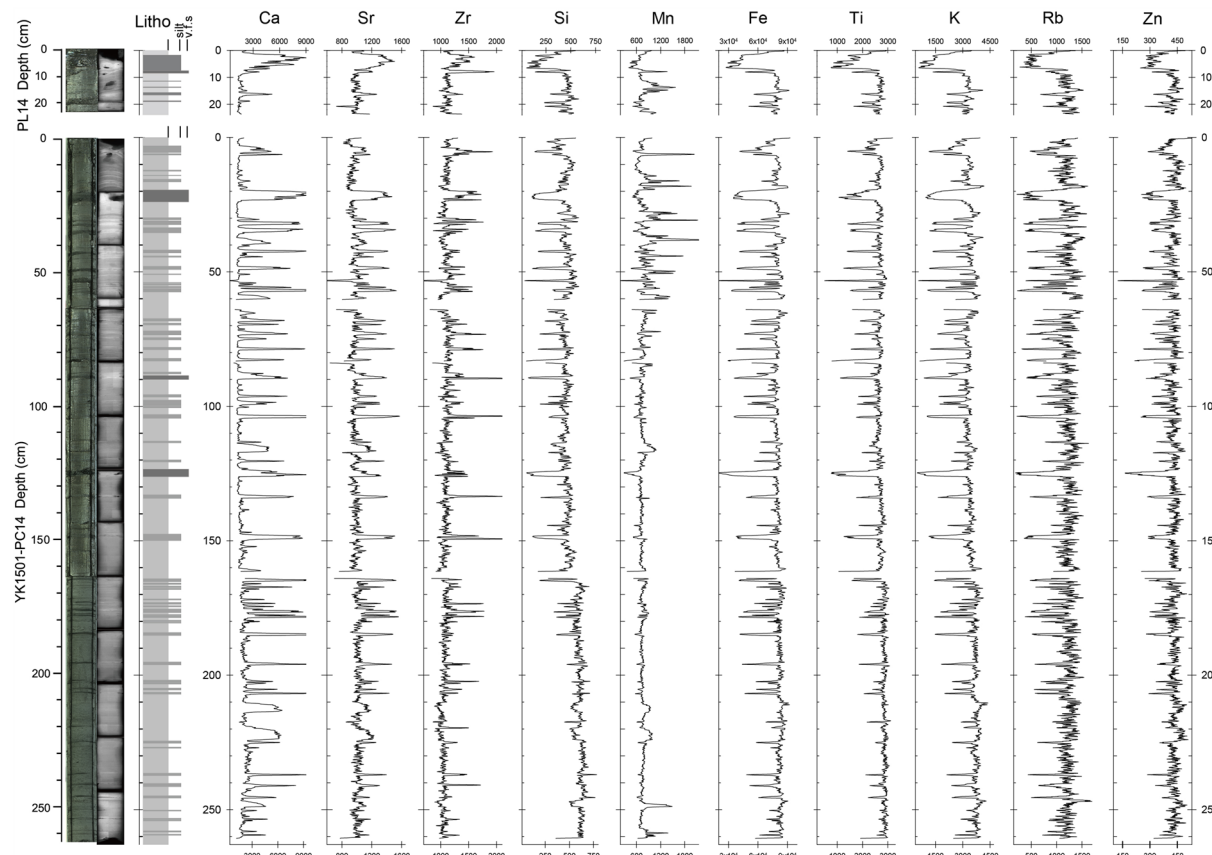


Fig. 2 ITRAX profiles of YK1501-PC14/PL14. Core photo, X-ray images, lithological column, and selected target elements from ITRAX of YK1501-PC14/PL14. We identified 60 turbidites (0.3–4.0 cm thick, average in 1.0 cm) based on visual core descriptions, X-ray images, element Ca intensity in the ITRAX profiles. Most of the thin turbidites can correlate to the positive peaks of the elements Ca, Sr, and Zr, and to the negative peaks of the Fe, Ti, K, and Rb

from the Taiwan orogenic belt during the Plio-Pleistocene and preserved in adjacent marine sedimentary basins (Horng and Roberts 2006; Horng et al. 2012). Low-temperature magnetometry can provide rapid identification of pyrrhotite in bulk samples based on its characteristic magnetic transition at ~ 35 K, known as the Besnus transition (Besnus and Meyer 1964; Rochette et al. 2011). In this study, we selected 13 discrete samples from PC14, 2 samples from PL14, 7 samples from 6K1467MG, and 8 samples from 6K1467MR. Each sample was approximately 200 mg in weight and was dried, stored in a capsule, and analyzed with a Magnetic Properties Measurement System (MPMS-XL5, Quantum Design) at the Center for Advanced Marine Core Research, Kochi University, Japan. Saturation isothermal remanent magnetization was imparted by a magnetic field of 3 T at room temperature (300 K) and its change was continuously measured while cooling from 300 to 10 K and warming back to 300 K in a zero magnetic field.

Radiocarbon dating and organic geochemistry analyses

We selected seven hemipelagic horizons from PC14 to determine radiocarbon ages from the dried bulk sediments. Radiocarbon dating was performed using accelerator mass spectrometry at Beta Analytic Co., Ltd. (Additional file 2: Table S2). Each dried sample (~ 1 g) of finely powdered sediment was washed with 1 N HCl at 80 °C to remove carbonates. Total organic carbon (TOC, wt. %), total nitrogen (TN, wt. %), and the stable carbon isotopic composition of TOC ($\delta^{13}\text{C}$, ‰ vs VPDB) were also analyzed for the seven horizons from YK1501-PC14 to compare to organic geochemical patterns in turbidites and hemipelagites from the southwestern end of Ryukyu Trench (i.e., PC04). The analyses were conducted at Geo-Science Laboratory, Japan (<https://www.geolab.co.jp/>).

Results and discussion

Lithology determined by visual core description and ITRAX elemental variations

The lithology of PC14/PL14 and PC04/PL04 is characterized by homogeneous gray mud layers intercalated with very thin-bedded fine sand layers (Fig. 2). Based on visual core description of PC14, X-ray images, and Ca intensity of the ITRAX profiles, we identified 60 turbidites ranging from 0.3 to 4.0 cm in thickness, with an average thickness of ~1.0 cm. Most of these turbidites are correlated with positive peaks of elements Ca, Sr, and Zr, as well as negative peaks of Fe, Ti, K, and Rb of ITRAX data (Fig. 2). Besides, similar baseline Ca/Fe ratios (~0.02–0.04) are evident in the hemipelagites of both PC14 and PC04 (Hsiung et al. 2021), except for the high-Ca mud intervals in PC14 (Fig. 2 and Additional file 5: Fig. S2). The lithology and ITRAX patterns of the push cores of 6K1467MG and 6K1467MR, which are located in the north of PL14/PC14, are similar to those of the pilot cores (Additional file 4: Fig. S1; redraw from Kawamura et al. 2023).

We observe the elemental correlations that Iron (Fe), titanium (Ti), and potassium (K) commonly found in clay minerals (Rothwell and Croudace 2015) exhibit a strong positive correlation coefficient (0.934 to 0.978). Besides, a moderate positive correlation between Si and Fe-Ti-K group ranges from 0.783 to 0.876. There is a moderate positive correlation (0.796) between Ca and Sr. It is noted that a relative low coefficient of Ca and Fe-Ti-K group (−0.218 to −0.399), suggesting that the negative peaks of Fe, Ti, and K vary due to the high concentration of Ca (Additional file 3: Table S3).

Based on the characteristics of the turbidites, where each turbidite has an average thickness of 1–2 cm and exhibits similar ITRAX patterns (positive peaks in positive Ca and negative Fe), we can infer that the turbidites of PC04 and PC14 are likely to have occurred under similar provenance of sediment. By comparing these profiles with those from the YK1611 push cores, we observe that 6K1467MR hemipelagites have higher Ca intensity (Additional file 4: Fig. S1). This variation in Ca intensity leads us to infer that PC04 and PC14 are essentially under similar source of sediments. However, it is also possible that 6K1467MR is partially affected by slumping from the north (Kawamura et al. 2023).

High calcium (Ca) and manganese (Mn) intervals

We highlight the five intervals of PC14 with relative high Calcium (high-Ca mud) at different depths: 58.5–60.1 cm, 113.7–117.1 cm, 210.2–213.9 cm, 221.7–224.0 cm, 246.7–248.9 cm (marked by yellow bars, Additional file 5: Figure S2). The lithology consists of

homogeneous gray mud, absence of prominent upper or lower boundaries. The thickness of high-Ca mud ranges from 1.65 to 3.75 cm, as determined by high-resolution ITRAX profiles. The high-Ca mud intervals are characterized by moderate to high Ca, Sr, and Mn concentrations. In particular, Ca intensity remains stable at around 5000 and can be easily distinguished from turbidite peaks. Comparing to the turbidite peaks, Fe intensity does not exhibit any significant variation in these intervals. Elemental variations in Ca and Mn in certain intervals may suggest alternative sediment sources. By comparing the ITRAX profiles, the high-Ca mud observed in PC14 are not present in PC04 (Hsiung et al. 2021). Despite the absence of submarine canyons or channels to provide sediment pathways across the Ryukyu forearc and forearc basins to the trench (Hsiung et al. 2017), the presence of normal hemipelagites and high-Ca mud indicates their possible sources from diverse areas. The high-Ca mud is potentially originating from the Ryukyu forearc. The presence of high-Ca mud at varying depths suggests that it is plausible a kind of event deposit.

Previous studies on marine sediments have demonstrated that the Ca/Fe ratio is a useful proxy for terrigenous components in sediments, and Zr/Rb is often positively correlated with mean grain size (Croudace et al. 2006; Rothwell and Croudace 2015). For example, the Ca/Fe ratio has been found to distinguish pelagic and re-deposited muds and assess textural character in turbidite-containing sequences in the western Mediterranean Sea (Rothwell et al. 2006). In cores PC14 and PC04, the Ca/Fe profiles demonstrate a close correspondence to the turbidite-hemipelagite sequence. Utilizing the same elemental ratios, the Zr/Rb vs. Ca/Fe plot of PC14/PL14 displays similar patterns (Fig. 3a). The enlarged plot of hemipelagites (gray circle) and high-Ca mud (green square) from Fig. 3a indicates that the Ca/Fe ratio of high-Ca mud ranges from 0.02 to 0.08 and Zr/Rb ranges from 0.8 to 1.0 (Fig. 3b). This consistency and focus in the plot suggest a steady sediment source(s). The Ca vs. Mn plot (Fig. 3c) reveals an irrelevant pattern for high-Ca mud and turbidites (represented by the red triangle), implying that the nature of high-Ca mud may differ from event deposits (e.g., muddy turbidites).

Magnetic parameters showing the characteristics of turbidites

Analytical results of magnetic parameters, including the minimum principal axis of the anisotropy of magnetic inclination (K_3) and K_m , were conducted throughout the cores of PL14/PC14 (Fig. 4). The K_3 directions are roughly the same in undisturbed sediments, except for the core tops of PL14 and PC14. Most of the K_m values in the cores of PL14/PC14 ranged from 1×10^{-4} and 4×10^{-4}

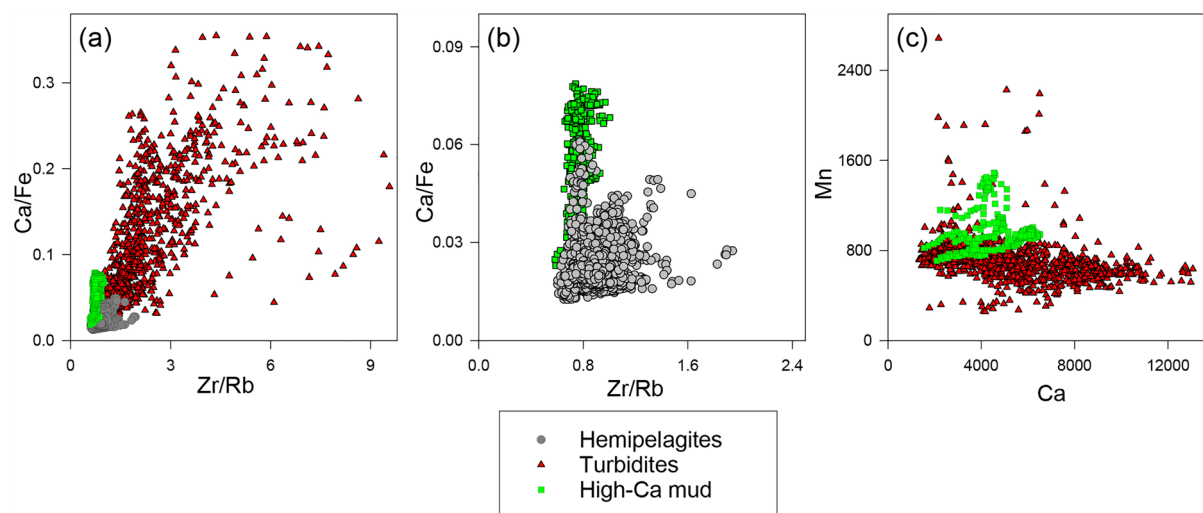


Fig. 3 Plots of elements ratios and intensities of ITRAX. **a** Plot of Zr/Rb vs. Ca/Fe of YK1501-PC14/PL14; **b** Enlarged plot of hemipelagites (gray circle) and high-Ca mud (green square) from (a). Ca/Fe of high-Ca mud ranges in 0.02–0.08 and Zr/Rb ranging in 0.8–1.0; **c** Plot of Ca vs. Mn for high-Ca mud and turbidites (red triangle)

SI units. In silt layers within turbidites, several peaks within the range of $\sim 7 \times 10^{-4}$ SI units were observed. These K_m peaks are evidently related to specific turbidites occurring throughout the entire downhole (Fig. 4). This phenomenon can be found in the cores PC14, PC04, and 6K1467MG. Although these K_m peaks correspond to specific turbidites with lower Fe values in ITRAX, the value of K_m is not only contributed by the iron compound, but also by the whole materials of the measured sediment sample. Therefore, the variation of Fe value in ITRAX could not correspond to that of K_m in this study.

AMS parameters are utilized to distinguish sediment fabric characteristics indicative of deposition and subsequent processes. Figure 2 illustrates the variation of AMS magnetic parameters with depth in cores P, F, L, and T. Profiles showed no significant downhole changes. The values of P and F in PL14/PC14 vary from 1.03 to 1.10 with depth. The P-value averages at 1.093, with a minimum of 1.014 and a maximum of 1.159. The P-values increase gradually with depth of sediments indicating a normal compaction effect of sediments (Fig. 4). The F value also averages with a minimum and maximum of 1.006 and 1.132, respectively. The generally low value of L (ranging from 1.01 to 1.02 throughout the cores) indicates magnetic mineral grains with a weak preferred orientation. The T values range from -0.624 to 0.998.

To perform a more comprehensive analysis of our AMS results, we generated plots of the shape parameter T versus P (Jelinek plot), the degree of lineation L versus F (Flinn-type plot), and the magnetic anisotropy parameter P as a function of the mean susceptibility K_m , grouped according to their lithology as either hemipelagites or

turbidites (Fig. 5). We determine a cube to be a turbidite if it contains turbidite layer(s), regardless of whether it is intermixed with hemipelagites. The plot of the PC04/PL04 shows more variability, suggesting imbrication of the sedimentary grains in PC14/PL14 is generally denser than PC04/PL04 (Fig. 5a and d). This result is consistent with core observation within thin turbidites in PC14/PL14. Both PC14/PL14 and PC04/PL04 exhibit an oblate fabric, with most of the lineation in the PC14/PL14 being less than 1.02 (Fig. 5b and e). Additionally, the K_m of turbidites shows slightly higher and more variable values compared to hemipelagites (Fig. 5c and f). This could be attributed to the fact that the cubes determined as turbidite comprise varying proportions of hemipelagites intercalated with thin-bedded turbidites. Consequently, the AMS fabric cannot provide turbidity flow direction in this study area. Besides, no preferred flow direction can be discernible from the whole AMS results in the PC14/PL14.

The low-temperature magnetometry results reveal that magnetite, which is evident by the characteristic transition at ~ 120 K (Verwey 1939), is the dominant magnetic carrier of the studied samples in this study area (Fig. 4 and Additional file 6: Fig. S3). Additionally, a low-temperature magnetic transition at ~ 35 K could be observed, which indicate the presence of pyrrhotite in the top sediments of PL14, PL04, and three turbidites of PC04 (Hsiung et al. 2021). The presence of pyrrhotite signatures in the top sediments of the two pilot cores suggests that sediment transport is active and spreading from the end of the Ryukyu Trench to the trench floor along the trench axis. Plot of low-temperature magnetic

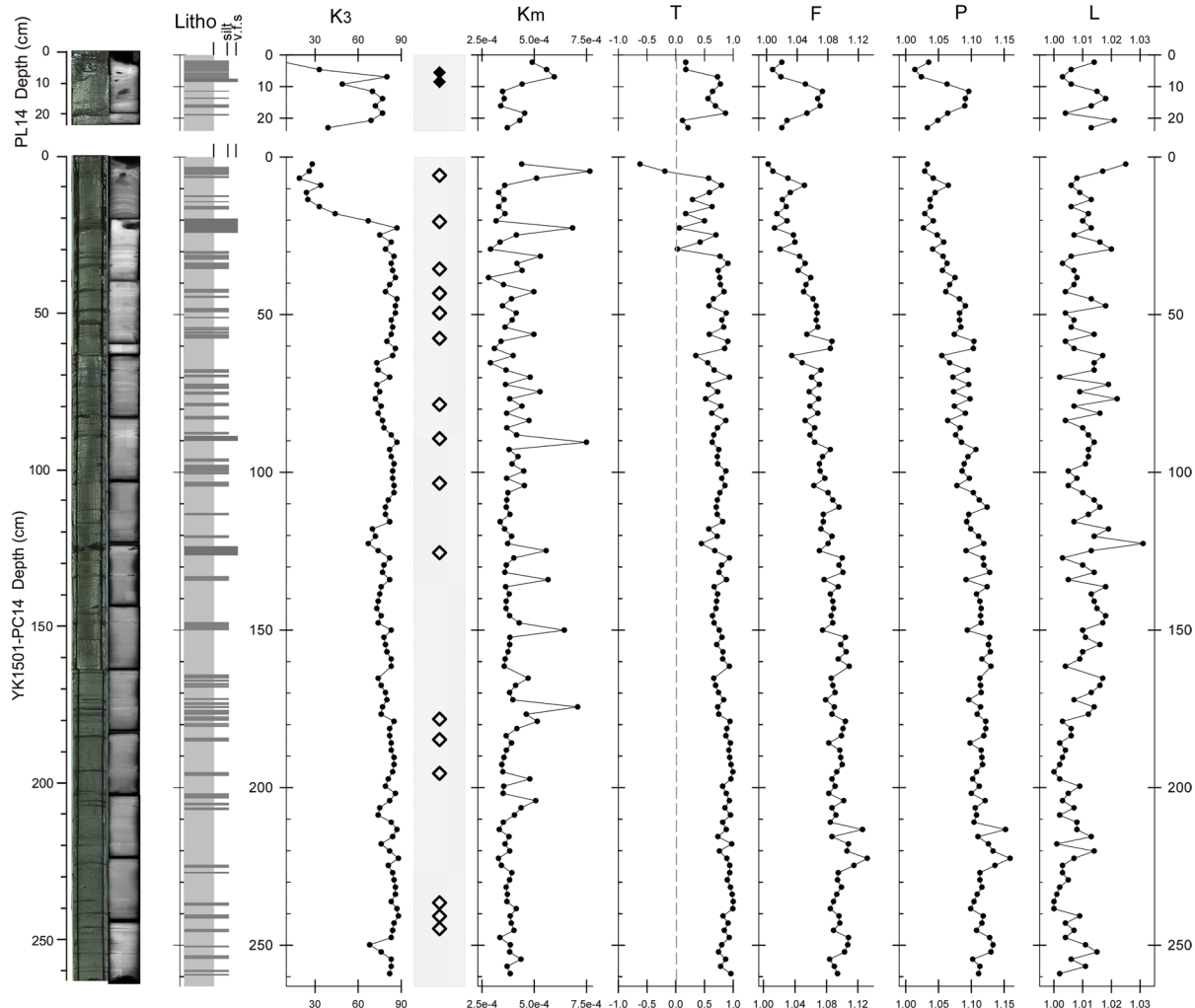


Fig. 4 Lithology and magnetic parameters of YK1501-PC14/PL14. Columns (from left to right) are core photograph, X-ray images, Lithological column, K_3 inclination, magnetic susceptibility (K_m). AMS parameters include: shape parameter (T), magnetic foliation (F), corrected anisotropy degree (P), and magnetic lineation (L). Solid diamonds in the column signals indicate the presence of both pyrrhotite (transition at ~ 35 K) and magnetite (~ 120 K), while open diamonds indicate magnetite only, as determined from the low-temperature magnetometry

analyses of bulk marine sediments from 8.5 cm depth in PL14 is provided for example (Additional file 6: Fig. S3). The absence of pyrrhotite signatures in PC14 and 6K1467MG/6K1467MR may be because of that pyrrhotite concentrations are too low to be not diagnostic in the low-temperature magnetometry. Another pertinent factor involves the consideration of sediment sources originating from the north, given the notable landslide to the north of site PC14. This observation implies that the hemipelagicites in PC14 might contain a relatively minor portion of forearc-sourced sediments.

The compaction process during diagenesis can still play a role, even in the case of a relatively short piston core like PC14, which is less than 3 m in length. However, the terrestrial pyrrhotite present in marine sediments

is relatively stable and less susceptible to the effects of diagenesis. Therefore, the preservation or alteration of pyrrhotite may not be significant.

Compiling the turbidite pattern of ITRAX and the presence of pyrrhotite signatures, we speculate that the turbidites in PC14 and PC04 may originate from the west (e.g., Taiwan).

In the case of turbidites in 6K1467MG, we observe positive Ca and negative Fe, without significant peak in K_m , which may be attributed to the relatively thin thickness of each turbidite (less than 2 cm). In a previous study, calcareous sand layers in the southern Ryukyu forearc exhibited negative peaks in K_m (Ikehara et al. 2022). Kawamura et al. (2023) suggested a paleo-flow direction from north to south based on AMS results, indicating

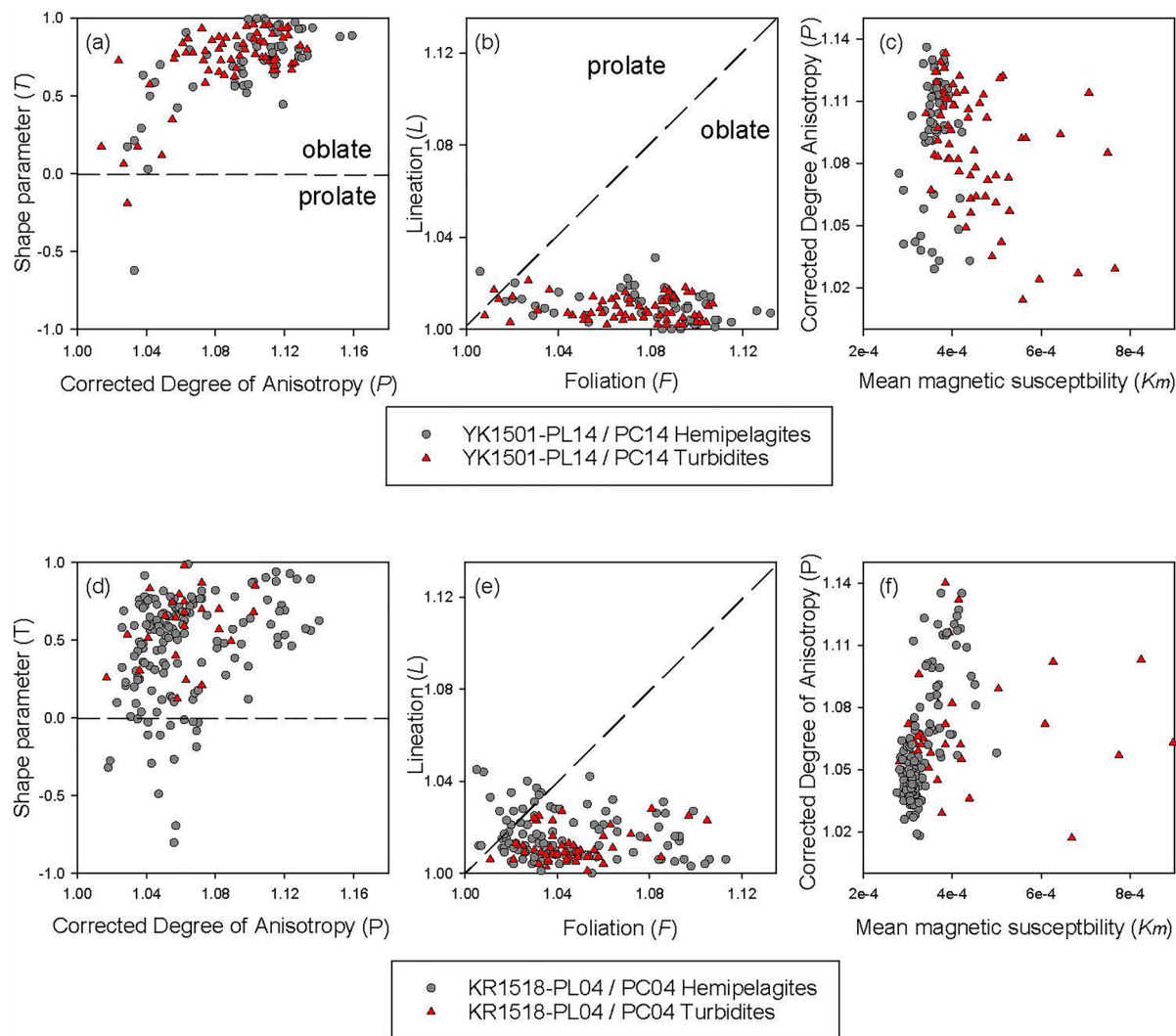


Fig. 5 AMS shape plots. AMS of YK1501-PC14/PL14 were in **(a, c, e)** and KR1518-PC04/PL04 in **(b, d, f)**, respectively. The correlation of shape susceptibility ellipsoid using the Jelinek plot **a, d**. Flinn-type diagrams **b, e** show oblate fabric. Degree of anisotropy vs. Mean susceptibility (**c, f**) show that turbidite layers (red triangle) are variable than that of hemipelagites (gray circle)

that the 6K1467MR sediments may originate from the north (e.g., forearc). Therefore, we speculate that the turbidites in 6K1467MG, between the site 6K1467MR and the PC14, likely originate from the north and/or west. In addition, no turbidites were identified in 6K1467MR (Additional file 4: Fig. S1).

Organic geochemistry and radiocarbon dating

Following a thorough examination of the lithology and ITRAX profiles of PC14, we have carefully selected seven depths in hemipelagic muds for radiocarbon dating, while avoiding turbidites. To compare these findings with those of PC04, we have selected the same depths for $\delta^{13}\text{C}$, TOC, and TN analyses. The purpose of this

selection is to validate whether our conclusions align with those of PC04 (Fig. 6). The seven samples exhibit $\delta^{13}\text{C}$ values ranging from -21.5 to $-20.0\text{\textperthousand}$, TOC concentrations ranging from 0.33 to 0.41 wt.%, and TN concentrations from 0.05 to 0.07 wt.%. The TOC/TN ratios range from 5.57 to 6.60. The seven radiocarbon measurements were obtained from bulk sediments of PC14, ranging from 17,680 to 26,710 ^{14}C yr BP in conventional age (Fig. 6a; Additional file 2: Table S2). The seven ages analyzed from hemipelagites exhibit zigzag trends with their stratigraphic depths.

When considering the conventional ages of PC04 in combination with the findings of PC14, the ^{14}C conventional age shows inconsistent. As a result, ^{14}C age

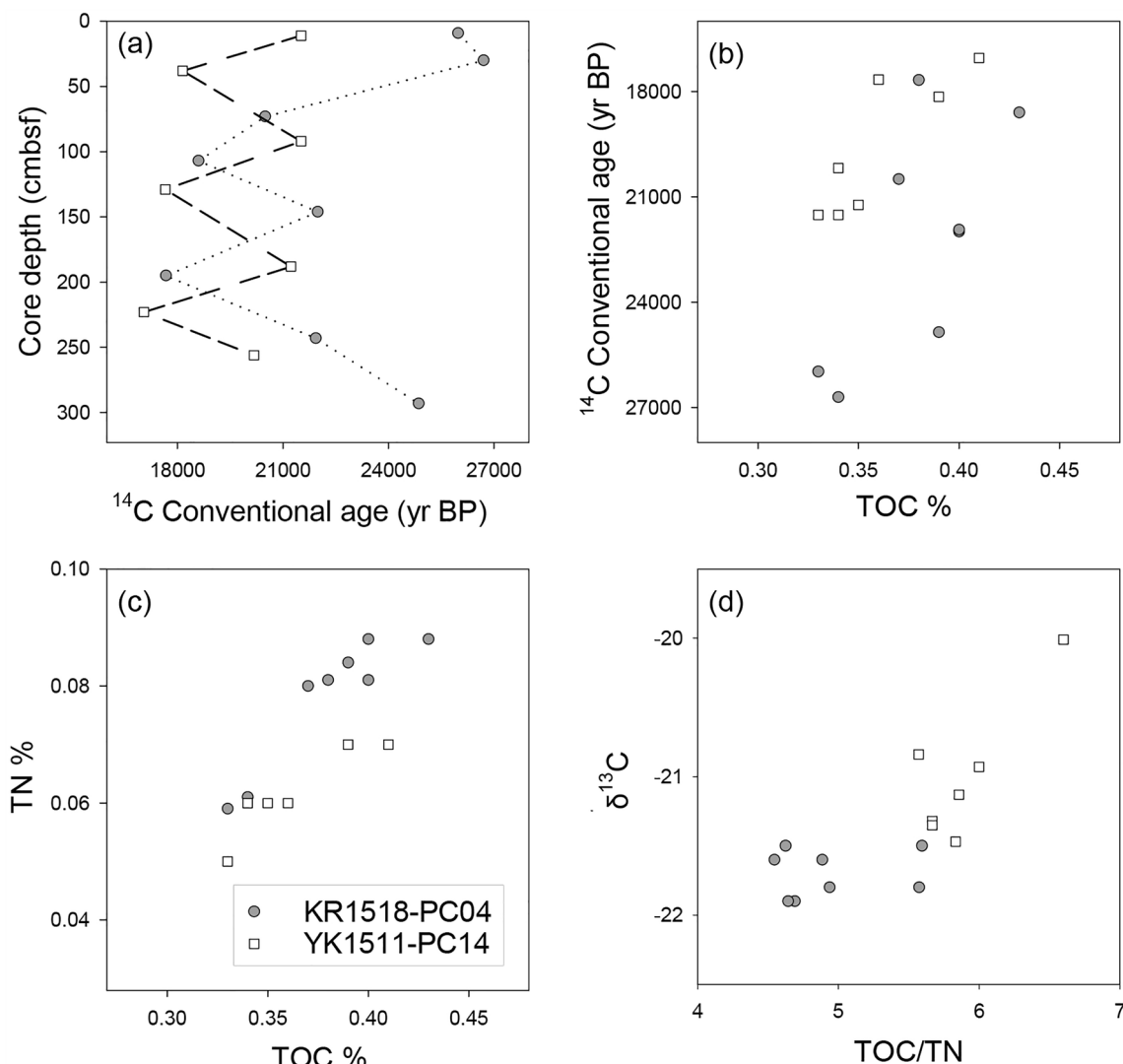


Fig. 6 Organic geochemistry results from YK1501-PC14/PL14 (square) and KR1518-PC04/PL04 (circle) based on their stable carbon isotopic compositions ($\delta^{13}\text{C}$), total organic carbon (TOC), and nitrogen (TN) contents. **a** Conventional radiocarbon ages of bulk sediments vs. core depth in centimeter below sea floor; **b** conventional radiocarbon ages vs. TOC; **c** TN vs. TOC; **d** $\delta^{13}\text{C}$ vs. TOC/TN

measurements from bulk sediments likely include older carbon without any systematic deviation. Unlike the radiocarbon conventional ages with an age model of the nearby Japan Trench (Schwestermann et al. 2021), the radiocarbon conventional ages of Ryukyu Trench's hemipelagic muds did not display a linear relationship with sediment depth. This disparity could be due to the abundance of old carbon in the hemipelagicites of PC14 and PC04. As a consequence, the dating results may not accurately reflect the true depositional ages of hemipelagic muds within this study area.

Sediment transport and sources of turbidites (event deposits) in the southwestern Ryukyu Trench

In PC14, we have identified 60 turbidites with thickness ranging from 0.3 to 4.0 cm (Fig. 2). The majority of these turbidites display planar and sharp bottom contacts, characterized by an extremely thin thickness of less than 1 cm. This suggests that these turbidites were likely initiated by relatively weak currents. Axial transport in the trench floor may be accomplished through flow and overbank spill in a current channel that runs along the landward wall, as previously proposed by Piper et al. (1973).

Previous studies have indicated that hyperpycnal flow, a type of turbidity current, which is considered to be slower and long-lived with estimated flow velocity of ~ 2 m/s and flow duration of several days or longer (Mulder et al. 2003; Nakajima 2006). This phenomenon could potential explain for turbidity currents transport sediments from the southwestern end of the Ryukyu Trench to its floor. Even the AMS results cannot provide clear turbidity flow direction, the presence of pyrrhotite in magnetic signatures provides further evidence of sediment transport along the Ryukyu Trench floor, with Taiwan-sourced sediments found at both the southwestern end of the Ryukyu Trench and the Ryukyu Trench floor.

Previous studies on marine sediments have demonstrated that the Ca/Fe ratio is a useful proxy for terrigenous components in sediments, and Zr/Rb is often positively correlated with mean grain size (Croudace et al. 2006; Rothwell and Croudace 2015). Intensity variations of Ca and Fe, effectively trace sedimentary provenance changes in the study area. The decreased Fe, a common phenomenon in upper X-ray fluorescence-scan profiles of organic-rich sediments, is likely due to the closed-sum effect of increased Ca (e.g. Löwemark et al. 2019). Considering the significant landslide to the north of PC14/PL14, we observe the similarities in element intensities and ratios from ITRAX to trace sedimentary provenances.

In the PC04 and PC14, a clear correlation between positive Ca and negative Fe peaks and turbidite show similarities to the climatic-driven turbidites (Fig. 8b of Lehu et al. 2016) on the continental slope offshore east Taiwan. Besides, the Ca/Fe ratio of hemipelagites in PC04 ranges around 0.02–0.04 (Fig. 9b, Hsiung et al. 2021), which is similar to that observed in PC14 (Fig. 3b). Moreover, plots of cores 6K1467MG and 6K1467MR display scattered and higher (~ 0.05) values compared to PC04 and PC14. Based on the consistent turbidite pattern and the similar Ca/Fe in hemipelagites in PC04 and PC14 (except for the high-Ca mud intervals), we assume that the sediments of PC14 and PC04 have the similar source(s). Cores 6K1467MG and 6K1467MR, located ~ 4 km away from PC14, could have received sediments contributed by the landslides from the north (Kawamura et al. 2023).

To constraint the potential turbidite occurrences of the Ryukyu Trench floor, the sedimentation rate of 2.42 mm/year from 6K1467MG (Kawamura et al. 2023) can be compared to the turbidites found in core PC14. The lowest turbidite in core PC14 was identified in a depth of 260 cm, implying the presence of turbidites in PC14 over the last thousand years. However, the sedimentation rate of 6K1467MG is roughly twice that of the Ryukyu Arc (Additional file 2: Table S2; Ujiie and Ujiie 1999). Ike-hara et al. (2022) provided two sedimentation rates of

hemipelagic mud from radiocarbon dates in 6.8 cm/ky (12 horizons of core YK1501-PC07) and 11.8 cm/ky (10 horizons of core YK1501-PC01). Significant differences in sedimentation rates suggest that the Ryukyu Arc sedimentation rates cannot refer to estimate turbidite recurrence in PC14.

Conclusion

This study presented very thin-bedded turbidites intercalated with hemipelagites in cores YK1501-PC14/PL14, obtained at 6,448 m water depth on the Ryukyu Trench floor. Three sediment types, turbidites, hemipelagites, and high-Ca mud were identified based on visual core descriptions of PC14, X-ray images, and Ca intensity of the ITRAX profiles. The contacts of 60 turbidites (0.3–4.0 cm thick) were determined based on Ca intensity. Most turbidites were less than 1 cm in thickness, displayed planar and sharp bottom contacts. Compiling the ITRAX of the turbidites from cores, we find that the characteristics of turbidites in PC14 and PC04 exhibit similarities, with positive peaks of elements Ca, Sr, and Zr, as well as negative peaks of Fe, Ti, K, and Rb. We can infer that the turbidites of PC04 and PC14 are likely to have occurred under similar settings. Besides, most hemipelagites in PC14 and PC04 mainly show similar ITRAX patterns, except that the five intervals in high-Ca mud in PC14 were observed through ITRAX. This implies that PC14 has an additional potential sediment source originating from the Ryukyu forearc. The AMS results in PC14/PL14 exhibit an oblate fabric, but cannot indicate the turbidity flow direction. In PL14, the presence of pyrrhotite in magnetic signatures provides indicated that Taiwan-sourced sediments may have been consistently dispersed as far as the southwestern Ryukyu Trench floor. This study enhances our understanding of the Ryukyu Trench turbidites and supports the concept of active sediment transport along the southwestern Ryukyu Trench.

Abbreviations

AMS	Anisotropy of magnetic susceptibility
K _m	Mean magnetic susceptibility
MPMS	Magnetic Properties Measurement System

Supplementary Information

The online version contains supplementary material available at <https://doi.org/10.1186/s40562-023-00303-9>.

Additional file 1: Table S1. Core information YK1501-PC14/PL14, KR1518-PC04/PL04, YK1611-6K1467MG, and 6K1467MR in this study.

Additional file 2: Table S2. Radiocarbon ages of core YK1501-PC14 compared to previous Conventional ^{14}C ages from the cores of the end of southwestern Ryukyu Trench and the Ryukyu Arc.

Additional file 3: Table S3. Correlation coefficient matrix of selected elements from ITRAX of the core YK1501-PC14.

Additional file 4: Figure S1. ITRAX of YK1611-6K1467MG and 6K1467MR. Core photo, X-ray images, lithological column, and selected target element profiles from ITRAX of the push cores YK1611-6K1467MG and 6K1467MR.

Additional file 5: Figure S2. Five intervals of high-Ca mud in various depths: 58.5–60.1 cm, 113.7–117.1 cm, 210.2–213.9 cm, 221.7–224.0 cm, 246.7–248.9 cm (marked in yellow bar). It is characterized in moderate high Ca, Sr, and Mn. There is no significant variation in Fe intensity in the five intervals. Note that void in 60.3–63.0 cm and 83.2–83.8 cm. This figure was set a break interval in 90–110 cm.

Additional file 6: Figure S3. MPMS magnetic susceptibility analyses of bulk marine sediments from 8.5 cm depth in YK1501-PL14 during **a** cooling and **b** warming over temperatures from 5 K to room temperature. Both heating and cooling rates were 3 K/min. *po*: pyrrhotite; *mt*: magnetite.

Acknowledgements

We gratefully recognize the efforts of the crew, and the marine technicians of Marine Work Japan Ltd. during the YK1501, KR1518, and YK1611 surveys. We also thank the operation teams of the Shinkai-6500 submersible during the YK1611 cruise. ITRAX measurements were performed as part of the cooperative research program of the Center for Advanced Marine Core Research, Kochi University, Japan (No. 17B062; No. 20B040).

Author contributions

KH, TK, and KI observed turbidites. TK analyzed paleomagnetic data of the cores and managed the cruise. MM helped for ITRAX measurements. YY helped for MPMS measurements. All authors contributed to scientific discussions and to the manuscript writing. All authors read and approved the final manuscript.

Funding

The YK1501 and KR1518 cruises were funded as part of the "Research Project for Compound Disaster Mitigation on the Great Earthquakes and Tsunamis around the Nankai Trough Region" by the Ministry of Education, Culture, Sports, Science and Technology of Japan. The analysis was funded by the JAMSTEC.

Availability of data and materials

Additional files 1, 2, 3, 4, 5, 6 are available. Correspondence and requests for materials should be addressed to KH.

Declarations

Competing interests

The authors declare that they have no competing interests' in this section.

Author details

¹Research Institute for Marine Geodynamics (IMG), Japan Agency for Marine-Earth Science and Technology (JAMSTEC), 2-15 Natsumisha-cho, Yokosuka 237-0061, Japan. ²Geological Survey of Japan, National Institute of Advanced Industrial Science and Technology (AIST), Tsukuba Central 7, 1-1-1 Higashi, Tsukuba 305-8567, Japan. ³Faculty of Agriculture and Marine Science, Kochi University, B200 Monobe, Nankoku, Kochi 783-8502, Japan.

⁴Marine Core Research Institute, Kochi University, B200 Monobe, Nankoku, Kochi 783-8502, Japan.

Received: 6 April 2023 Accepted: 8 October 2023

Published online: 18 October 2023

References

- Angelier J (1986) Geodynamics of the Eurasia-Philippine Sea Plate Boundary: preface. *Tectonophysics* 125(1–3):IX–X
- Besnus MJ, Meyer AJP (1964) Nouvelles données expérimentales sur le magnétisme de la pyrrhotine naturelle. In: Proceedings of the International Conference on Magnetism. Nottingham, p. 507–511.
- Croudace IW, Rindby A, Rothwell RG (2006) ITRAX: description and evaluation of a new multi-function X-ray core scanner. *Geol Soc Lond Spec Publ* 267(1):51–63
- Hornig CS, Huh CA (2011) Magnetic properties as tracers for source-to-sink dispersal of sediments: a case study in the Taiwan Strait. *Earth Planet Sci Lett* 309(1–2):141–152
- Hornig CS, Roberts AP (2006) Authigenic or detrital origin of pyrrhotite in sediments?: resolving a paleomagnetic conundrum. *Earth Planet Sci Lett* 241:750–762. <https://doi.org/10.1016/j.epsl.2005.11.008>
- Hornig CS, Huh CA, Chen KH, Lin CH, Shea KS, Hsiung KH (2012) Pyrrhotite as a tracer for denudation of the Taiwan orogen. *Geochem Geophys Geosyst* 13(8):Q08Z47
- Hsiung KH, Kanamatsu T, Ikebara K, Shiraishi K, Hornig CS, Usami K (2017) Morpho-sedimentary features and sediment dispersal systems of the southwest end of Ryukyu Trench: a source-to-sink approach. *Geo Mar Lett* 37(6):561–577
- Hsiung KH, Kanamatsu T, Ikebara K, Usami K, Hornig CS, Ohkouchi N, Ogawa NO, Saito S, Murayama M (2021) X-ray fluorescence core scanning, magnetic signatures, and organic geochemistry analyses of Ryukyu Trench sediments: turbidites and hemipelagites. *Prog Earth Planet Sci* 8:2. <https://doi.org/10.1186/s40645-020-00396-2>
- Ikebara K, Usami K, Kanamatsu T, Arai K, Yamaguchi A, Fukuchi R (2018) Spatial variability in sediment lithology and sedimentary processes along the Japan Trench: use of deep-sea turbidite records to reconstruct past large earthquakes. *Geol Soc Lond Spec Publ* 456(1):75–89
- Ikebara K, Kanamatsu T, Usami K (2022) Possible tsunami-induced sediment transport from coral reef to deep sea through submarine canyons on the southern Ryukyu Forearc, Japan. Source or Sink? Erosional and depositional signatures of tectonic activity in deep-sea sedimentary systems. *Front Earth Sci* 10:753583. <https://doi.org/10.3389/feart.2022.753583>
- JAMSTEC (2015) YOKOSUKA YK15-01 cruise data. JAMSTEC, Yokosuka. <https://doi.org/10.17596/0001656>
- JAMSTEC (2016) KAIREI KR15–18 cruise data. JAMSTEC, Yokosuka. <https://doi.org/10.17596/0001656>
- Karig DE (1973) Plate convergence between the Philippines and the Ryukyu Islands. *Mar Geol* 14(3):153–168. [https://doi.org/10.1016/0025-3227\(73\)90025-X](https://doi.org/10.1016/0025-3227(73)90025-X)
- Kawamura K, Oguri K, Inoue M, Hsiung KH, Kudaka T, Takai K (2023) Ongoing persistent slope failures at the toe of a giant submarine slide in the Ryukyu Trench that generated the AD 1771 Meiwa Tsunami. In: Alcántara-Ayala I et al (eds) Progress in landslide research and technology, volume 1, issue 2, 2022. Springer, Cham. https://doi.org/10.1007/978-3-031-18471-0_5
- Lehu R, Lallemand S, Ratkov G, Babonneau N, Hsu SK, Lin AT, Dezileau L (2016) An attempt to reconstruct 2700 years of seismicity using deep-sea turbidites offshore eastern Taiwan. *Tectonophysics* 692:309–324
- Löwemark L, Bloemsma M, Croudace I, Daly JS, Edwards RJ, Francus P, Galloway JM, Gregory BRB, Huang JJS, Jones AF KM, Luo Y, MacLachlan S, Ohlendorf C, Patterson RT, Pearce C, Profe J, Reinhardt EG, Stranne C, Tjallingii R, Turner JN (2019) Practical guidelines and recent advances in the Itrax XRF core scanning procedure. *Quat Int* 514:16–29
- Malatesta C, Gerya T, Crispini L, Federico L, Capponi G (2013) Oblique subduction modelling indicates along-trench tectonic transport of sediments. *Nat Commun* 4:2456
- Mulder T, Syvitski JP, Migeon S, Faugères JC, Savoye B (2003) Marine hyperpycnal flows: initiation, behavior and related deposits: a review. *Mar Pet Geol* 20(6–8):861–882
- Nakajima T (2006) Hyperpycnites deposited 700 km away from river mouths in the central Japan Sea. *J Sediment Res* 76(1):60–73
- Oguri K, Masqué P, Zabel M, Stewart HA, MacKinnon G, Rowden AA, Berg P, Wenzhöfer F, Glud RN (2022) Sediment accumulation and carbon burial in four hadal trench systems. *J Geophys Res* 127(10):e2022JG006814
- Okamura Y, Nishizawa A, Fujii Y, Yanagisawa H (2018) Accretionary prism collapse: a new hypothesis on the source of the 1771 giant tsunami in the Ryukyu Arc, SW, Japan. *Sci Reps* 8(1):13620
- Pickering KT, Hiscott RN (2015) Deep marine systems: processes, deposits, environments, tectonics and sedimentation. John Wiley & Sons, Hoboken

- Piper DJW, von Huene R, Duncan JR (1973) Late Quaternary sedimentation in the active eastern Aleutian Trench. *Geology* 1(1):19–22
- Rochette P, Fillion G, Dekkers MJ (2011) Interpretation of low-temperature data Part 4: the low-temperature magnetic transition of monoclinic pyrrhotite. *IRM Q* 21(1):1–11
- Rothwell RG, Croudace IW (2015) Twenty years of XRF core scanning marine sediments: what do geochemical proxies tell us? In: Croudace IW, Rothwell RG (eds) *Micro-XRF studies of sediment cores*. Springer, Dordrecht, pp 25–102
- Rothwell RG, Hoogakker B, Thomson J, Croudace IW, Frenz M (2006) Turbidite emplacement on the southern Balearic Abyssal Plain (western Mediterranean Sea) during Marine Isotope Stages 1–3: an application of ITRAX XRF scanning of sediment cores to lithostratigraphic analysis. In: Rothwell RG (ed) *New techniques in sediment core analysis*, vol 267. Geological Society Special Publication, London, pp 79–98
- Schwestermann T, Eglington TI, Haghipour N, McNichol AP, Ikehara K, Strasser M (2021) Event-dominated transport, provenance, and burial of organic carbon in the Japan Trench. *Earth Planet Sci Lett* 563:116870
- Ujiie H, Ujiie Y (1999) Late Quaternary course changes of the Kuroshio Current in the Ryukyu Arc region northwestern Pacific Ocean. *Mar Micropaleontol* 37(1):23–40. [https://doi.org/10.1016/S0377-8398\(99\)00010-9](https://doi.org/10.1016/S0377-8398(99)00010-9)
- Verwey E (1939) Electronic conduction of magnetite (Fe_3O_4) and its transition point at low temperatures. *Nature* 144:327–328. <https://doi.org/10.1038/144327b0>

Publisher's Note

Springer Nature remains neutral with regard to jurisdictional claims in published maps and institutional affiliations.

Submit your manuscript to a SpringerOpen® journal and benefit from:

- Convenient online submission
- Rigorous peer review
- Open access: articles freely available online
- High visibility within the field
- Retaining the copyright to your article

Submit your next manuscript at ► springeropen.com